DETERMINATION OF THE EFFICIENCY OF A COOLED TURBINE STAGE TESTED IN A COMPRESSION TUBE FACILITY

L. Porreca, R. Dénos
von Karman Institute for Fluid Dynamics
Chaussée de Waterloo, 72
1640 Rhode Saint Genèse, Belgium
contact: denos@vki.ac.be

ABSTRACT

This work intends to determine with a good accuracy the efficiency of a cooled turbine stage tested in a compression tube facility. Due to the uncertainty associated with gas temperature measurements, the mechanical method is preferred to the thermodynamic method.

The determination of the stage mass flow is presented in a separate paper by Porreca and Dénos, 2002.

The shaft power is derived from the rotor acceleration during the blowdown and from the rotor inertia. An experimental technique is described to evaluate the inertia. A method is also proposed to estimate the mechanical losses. Then the contribution of the heat transferred to the blades and the endwalls during the blowdown is analyzed. The influence of the coolant flows in the determination of the incoming enthalpy is evaluated.

Finally, the method is applied to a number of tests. The resulting uncertainty on the efficiency for each test is equal to +/- 1.44 % and the test-to-test repeatability is of the same order. A further reduction of the uncertainty can be achieved by improving the accuracy on the stage downstream total pressure and on the rotor acceleration during the blowdown.

INTRODUCTION

The measurement of turbine stage efficiency is of primary importance to evaluate the benefits resulting from new designs or determine the stage operating conditions at off-design.

The efficiency is defined as the ratio between the real power delivered by the turbine and the maximum power available from the fluid when achieving an isentropic expansion. In the thermodynamic method, the real power is determined thanks to stage downstream temperature traverses. In the mechanical method, the real power is evaluated form torque measurements on the shaft. The mechanical method is often preferred because it is usually more accurate and avoids time-consuming probe traverses. In both methods however, the power available from an isentropic expansion is usually evaluated from the mass flow, stage inlet temperature traverses and stage downstream pressure traverses.

The efficiency of a turbine stage is often determined in continuously running facilities operating under steady conditions and under thermal equilibrium.

In a compression tube facility, testing times are very short (~0.3 s) and the turbine does not operate under thermal equilibrium. It is of course a challenge to determine all the above-mentioned quantities in such a short time.

In the literature, the contributions to this problem are rather scarce because of the small number of short duration facilities. Guenette et al., 1989, showed that aerodynamic turbine performance can be measured in short duration facility using corrections for the fact that the test is not performed under an adiabatic regime. Keogh et al., 2000 and 2002, present techniques to evaluate the mass flow and the shaft torque. They calculate the turbine efficiency taking into account the influence of the coolant flows.

This paper focuses on the accurate evaluation of the turbine stage efficiency tested in the VKI CT-3 facility. In a companion paper, Porreca and Dénos, 2002, present a method to evaluate the mass flow in this test rig.

The turbine power is derived from the acceleration of the rotor during the blowdown and the inertia of the rotating parts. The inertia of the rotor is determined by monitoring the rotor acceleration when applying a known torque.

Then the mechanical losses are evaluated. A mathematical model is used to predict the different losses due to the bearing friction, the windage of the blades and the disk ventilation. The coefficients of the model are fitted to match an experiment where the rotor decelerates freely under varying

pressure. Afterwards, the heat transferred from the fluid to the endwalls is estimated. The influence of the stator and rotor coolant flows is also analyzed.

The overall procedure is finally applied to a number of tests.

NOMENCLATURE

C_p	specific heat at constant pressure
C	chord
g	gravitational constant
h	convective heat transfer coefficient
I_r	rotor moment of inertia
I_p	pulley moment of inertia
m	mass
$\dot{m}$	mass flow
Nu	Nusselt number
p	pressure
P	power
$\dot{q}$	heat flux
R	gas constant
R_r	rotor radius
S	surface, area
k	conductive heat transfer coefficient
T	temperature
Tr	torque
u,w,v	peripheral, relative and absolute velocity
Greek	
ΔE	change of energy
$\theta, \dot{\theta}, \ddot{\theta}$	angular position, velocity and acceleration
π	stage pressure ratio p_{01}/p_{03}
ρ	gas density
η	efficiency
Subscript	
0	total quantity
1	stage inlet plane
2	stator exit plane
3	stage exit plane
4	2nd stator exit plane
ax	axial
Cool	coolant flows
Comp	compression
frict	friction
Heat	heat transfer
is	isentropic
Loss	losses
mech	mechanical
r	relative frame, rotor
RotCool	rotor coolant flow
S	stator
Sh	shaft
Vent	ventilation
Wind	windage

THE TRANSONIC AXIAL TURBINE STAGE, THE TEST RIG

The high-pressure turbine stage under investigation is composed of 43 vanes and 64 blades. Detailed investigations were carried out previously focusing on the time-averaged and time-resolved aero thermal flow in the stage (Dénos et al. 2001, Paniagua et al., 2001, Didier et al., 2002). The vanes are internally cooled and the coolant flow is ejected at the trailing edge on the pressure side. The vane coolant mass flow rate amounts to 3% of the mainstream mass flow. The rotor is film-cooled. Flow ingress or leak exists in between the stator and the rotor platforms at hub depending on the pressure inside the hub cavity. The design rotational speed of the stage is 6500 RPM. Typical test conditions are reported in Table 1. In this investigation, tests for two different rotor coolant flow rates will be processed.

Test conditions	Re_{2c}	P_0 *(bar)*	T_0 *(K)*	P/p
Re high, P/p nom	$1.26 \cdot 10^6$	2.22	480	3.08
'0% cooling'	no rotor coolant flow			
'3% cooling'	0.78 % of stage mass flow in rotor			

Table 1: Operating conditions

The turbine stage is tested in the VKI compression tube turbine test rig (see Sieverding and Arts, 1992). The Reynolds number and stage pressure ratio are representative of those encountered in modern aero-engines. Prior to the test, the rotor is spun-up under vacuum to almost design speed. The compression tube provides then a blowdown of hot gas on the cold turbine stage simulating heat transfer to the blades and endwalls with a realistic T_{gas}/T_{wall} temperature ratio. Constant flow conditions are maintained during ~0.3 s. The delivered power is converted into kinetic energy through an acceleration of the rotor. An inertia wheel limits the rate of acceleration. More details on the operating principle can be found in the companion paper by Porreca and Dénos, 2002.

TURBINE EFFICIENCY DEFINITION

The turbine efficiency is defined as the real power delivered by the fluid to the turbine divided by the maximum power available from the fluid i.e. through an isentropic expansion:

$$\eta = \frac{P_{RealExpansion}}{P_{PerfectExpansion}} \qquad (1)$$

A control domain can be defined taking into account the turbine stage as shown in Figure 1. The control domain, represented by dotted line, begins $0.5\,C_{Sax}$ upstream of the stator blade leading edge (plane 1) and ends $0.5\,C_{Rax}$ downstream of the rotor blade trailing edge (plane 3). Planes 1 and 3 correspond to the measurement planes where probe traverses are performed. The stage is fed by the main flow coming from the settling chamber, while there is a internal coolant flow leaving the stator trailing edge and a film cooling flow on the rotor

blades. Additionally, there is a cavity flow exiting the slot that is located between the stator and the rotor at hub. In plane 1, equal dimensionless total pressure and temperature profiles are measured for all the test conditions.

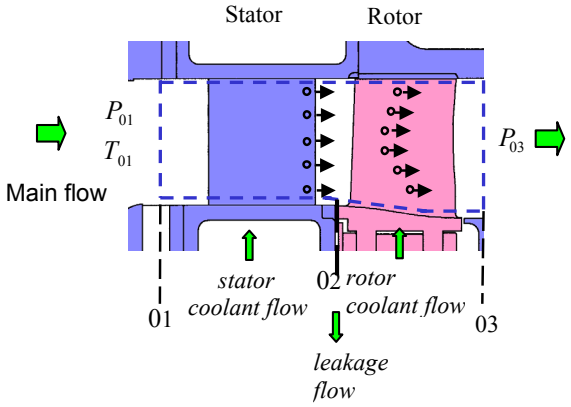

Figure 1: Turbine stage control domain

On this control domain, the denominator of the efficiency (equation 1) can be expressed as:

$$P_{\substack{Perfect\\Expansion}} = P_{Isen} + P_{heat} = \left[\iint_{Surface01} \dot{m}_{Stator} C_p T_{01} ds + \dot{m}_{Cool} C_p T_{Cool} \right] - \left[\iint_{Surface03} \dot{m}_{Stator} C_p T_{03,is} ds + \dot{m}_{leaks} C_p T_{leaks} \right] + P_{heat} \quad (2)$$

The isentropic stage exit temperature $T_{03,is}$ can be derived from traverses of total pressure and total temperature at stages inlet and traverses of total pressure at stage exit: $T_{03,is} = T_{01}\left(\frac{P_{03}}{P_{01}}\right)^{\frac{\gamma-1}{\gamma}}$

The real power can be expressed as:

$$P_{\substack{Real\\Expansion}} = P_{\substack{Real\\Adiabatic}} + P_{Heat} = \iint_{Surface01} \dot{m}_{stator} C_p T_{01} ds - \iint_{Surface03} \dot{m}_S C_p T_{03} ds \quad (3)$$

Note that a term linked to heat transfer P_{heat} appears in both numerator and denominator. Indeed, during the blowdown, the fluid heats up the blades and the endwalls, initially at ambient temperature. This heat is subtracted from the fluid and does not contribute to the expansion process, whether perfect or real. For this reason, this amount of heat is added to the heat extracted by expansion in both perfect and real process. The assumption here is that the same amount of heat is extracted during the perfect expansion and the real one which is an approximation.

The real power $P_{\substack{Real\\Expansion}}$ can be evaluated with the thermodynamic method or the mechanical method. In the thermodynamic method, the stage exit temperature T_{03} distribution and the mass flow distribution are required. If one simplifies the expression of the efficiency, neglecting coolant flows and heat transfer, and considering constant distribution over the inlet and outlet surfaces, equation (1) can be written as $\eta = \frac{C_p(T_{01} - T_{03})}{C_p(T_{01} - T_{03is})}$

In the turbine stage under analysis, the temperature drop $T_{01} - T_{03}$ is of the order of 100 K. This means that a relative uncertainty of 0.5% requires an absolute uncertainty on the total temperature difference of 0.5 K. Up to now, the thermocouples used in the typical conditions of the blowdown test do not allow reaching such a small uncertainty mainly due to transient conduction.

For this reason, the mechanical method is preferred. Because one wants to determine a pure aerodynamic efficiency, it should not depend on heat transfer, mechanical losses or windage on the disc. The real power should be expressed as:

$$P_{\substack{Real\\Expansion}} = (P_{sh} + P_{mech} + P_{wind}) + P_{heat} \quad (4)$$

In order to compute the efficiency using values measured at mid-span only, the following simplified equation will be used:

$$\eta = \left(P_{Sh} + P_{mech} + P_{wind} + P_{Heat}\right) \Big/ \left\{ \dot{m}_S c_p T_{01} \left[1 - \left(\frac{P_{03}}{P_{01}}\right)^{\frac{\gamma-1}{\gamma}} \right] + \dot{m}_{Cool} Cp \Delta T_{0Cool} + \dot{m}_{Leak} Cp \Delta T_{0Leak} + P_{heat} \right\} \quad (5)$$

In contrast to the thermodynamic method, the terms in equation 4 represent global quantities and, hence, require less effort to acquire than full thermocouple area traverses, especially in the case of a short duration facility.

DETERMINATION OF THE EFFICIENCY

Mass flow

The stage mass flow is a key quantity in the determination of the denominator of the efficiency (equation 2). It is derived thanks to a model of the blowdown facility that reproduces accurately the measured pressure and temperature at several locations of the test rig (see Porreca and Dénos, 2002). The results present an uncertainty of 0.88% and 1.6% for a single experiment depending on the test conditions. For the configuration that will be investigated here, the highest uncertainty is achieved as shown in Table 2.

Condition	Stage mass flow [kg/s]
0% rotor cooling	15.27
3% rotor cooling	15.36
Uncertainty	+/- 1.6 %
Dispersion	+/- 0.40 % (20:1)

Table 2: Mass flow results for 1 and ½ stage configuration test rig.

Work is under progress to reduce it. Consequently, the uncertainty on the efficiency will be at least of this level. However, the test-to-test dispersion is much smaller (0.4 %), i.e. the uncertainty is mainly due to a systematic error. This means that although the absolute value of the efficiency is not accurate, small variations of efficiency can still be measured.

Shaft Power

The turbine test rig is not equipped with a power absorption system. During the blowdown, the rotor accelerates at a rate $\ddot{\theta}$ and the mechanical power can be derived from $P_{sh} = I_r \ddot{\theta}\dot{\theta}$. The rotational speed is measured thanks to a diode that delivers one pulse per rotor revolution. In addition, an accurate knowledge of the inertia is required.

-Principle

The method consists in applying a known torque *Tr* to the rotor and recording the angular acceleration. Assuming no friction, the momentum of inertia is equal to $I_r = Tr/\ddot{\theta}$. In presence of friction losses (bearings), the absorbed energy can be expressed as:

$$\Delta E_{frict} = \int F_r dx$$

This integral is very difficult to evaluate. Haldeman and Dunn (1996) replaced this term with an averaged value which will be the same in a given speed range.

$$\Delta E_{frict} = \int F_r dx \approx \overline{F}_r \left(\theta_{final} - \theta_{initial}\right)$$

If an acceleration/deceleration test is performed during which the losses are assumed to be equal during the two phases of the test, this term can be eliminated. This is achieved as follows. The rotating assembly (turbine disc, inertia wheel, shaft and bearing casing) is attached to a mass via a string and a pulley. An encoder monitors the angular position (see Figure 2).

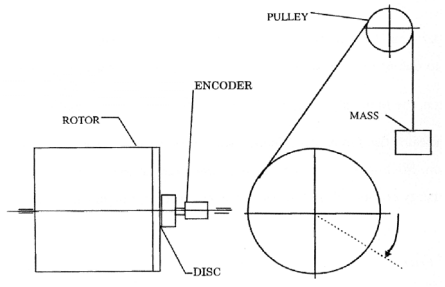

Figure 2: Sketch of the experimental set-up

During the first phase, the turbine rotor is accelerated by the weight until the mass touches the ground. The instant at which the mass touches the floor is determined thanks to an electrical contact. In the second phase, the mass is on the floor and the rotor decelerates freely under the influence of the bearing friction. Different masses can be used to check the validity of the method.

-Physical model

As explained in Haldeman and Dunn (1996), the governing equations of the two phases of the experiments are:

1) during the rotor acceleration (*a* to *b*),

$$\Delta E_{potential} = \Delta E_{kinetic} + Friction$$

$$Rmg\left(\theta_b - \theta_a\right) = \overline{F}_r\left(\theta_b - \theta_a\right) + \left(I_R + mR^2 + I_P \frac{R^2}{r^2}\right)\frac{\left(\dot{\theta}_b^{\,2} - \dot{\theta}_a^{\,2}\right)}{2}$$

2) during the rotor deceleration (*c* to *d*),

$$0 = \Delta E_{Kinetic} + Friction$$

$$0 = \overline{F}_r\left(\theta_c - \theta_d\right) + \left(I_R\right)\frac{\left(\dot{\theta}_c^{\,2} - \dot{\theta}_b^{\,2}\right)}{2}$$

After eliminating the friction term, it appears that the inertia can be determined from only 2 coefficients provided by the quadratic regression of the angular history during the acceleration ($a_{acc}\theta^2$) and deceleration ($a_{dec}\theta^2$) phases. This is valid only if the angular velocity is similar in the two phases. The inertia can then be expressed as:

$$I_R = \frac{R_r m\left(g - 2a_{acc}R_r - \dfrac{2I_P R_r a_{acc}}{mr^2}\right)}{2\left(a_{acc} - a_{dec}\right)}$$

A dedicated Fortran routine was written to evaluate accurately the quadratic coefficients on two portions (acceleration and deceleration) of similar angular velocities. The technique was validated on different portion widths and for different masses (Paniagua 1997).

-Inertia results

The results are presented in Table 3 together with the test-to-test dispersion reported as a standard deviation on a basis of 16 tests. An uncertainty analysis was also carried out for a single test (see Table 4). The most sensitive parameters are the a_2 and *b,* the coefficients that are used to fit the quadratic law.

The resulting uncertainty for a single test is equal to 1.85 %. Here again, the test-to-test repeatability is better than the uncertainty, i.e. part of the uncertainty can be attributed to a systematic error. As the same value of the inertia will be used for all the tests, this will not affect the possibility of measuring efficiency changes, although the absolute value may not be as accurate as wanted.

	a_2	b_2	*Inertia [kg*m²]*
Mean	0.2474	-0.1509	*17,7153*
Standard dev	0.001873	0.000724	0,072
% to the mean	0.757	0.480	0.41

Table 3: Inertia results.

Parameter	*mean*	*uncertainty %*	ΔI_r %
R [m]	0.2924	0.017	0.016
Mass [Kg]	5001.1	0.022	-0.016
r [m]	0.0736	0.872	0.001
g [m/s²]	9.8066	0.034	0.033
a_2	0.2474	1.483	-0.971
b_2	0.1509	-0.941	1.306
I_p *[Kg*m²]*	0.00162	1.851	-0.358

Table 4: Rotor inertia uncertainty analysis for a single test

-Power results

Values of shaft power are reported in Table 5 for two rotor film-cooling rates. The nominal power of 1.52 MW slightly decreases when the rotor is film-cooled. In reality, this power decrease is mainly due to a change of stage pressure ratio rather than a change in efficiency.

	0% condition	*3% condition*
Acc [rpm/s²]	1154.6	1123.6
Power [W]	1526.2	1488.7
St. dev	19.01	21.94
%	1.24	1.95
Nb of test	12	11

Table 5: Shaft power results.

Mechanical and windage losses.

The terms $P_{mech} + P_{wind}$ in equation 4 are now evaluated. These terms consist in the power lost in the rotor bearings and in the air friction on the rotor disc (disc windage) and blades (ventilation).

Correlations that can predict the magnitude of ventilation and disc windage losses can be found in the literature (Traupel, 1958). Bearing manufacturers also provide loss predictions. However, one cannot rely on correlations established under specific conditions. Thus, an experimental determination is preferred.

For this purpose, free decelerations under varying pressure were performed. The kinetic energy of the rotor decreases under the influence of mechanical, windage and ventilation losses. Because windage and ventilation losses depend on both pressure and rotational speed but mechanical losses depend only on the rotational speed, the variation of pressure should allow to quantify separately the two types of losses. Indeed, during a real test, disc windage losses are present but there is no ventilation in the blades.

$$P_{loss} = P_{mech} + P_{wind} \qquad (6)$$

where:

$$P_{wind} = P_{disk} + P_{vent}$$

The torques associated with each type of losses can be expressed as:

$$Tr_{mech} = C_{mech}\dot{\theta}^{N_{mech}}$$

$$Tr_{vent} = \rho C_{vent}\dot{\theta}^{N_{vent}} \qquad (7)$$

$$Tr_{disk} = \rho C_{disk}\dot{\theta}^{N_{disk}}$$

Hence, the total rotor torque is equal to:

$$Tr = Tr_{mech} + Tr_{vent} + Tr_{wind} \qquad (8)$$

and the deceleration of the rotor can be computed with $\ddot{\theta} = Tr/I_r$. A test is performed where the rotor is spun-up to design speed under ~0.1 bar. Then the rotor decelerates freely while the pressure increases in the test section (see Figure 3).

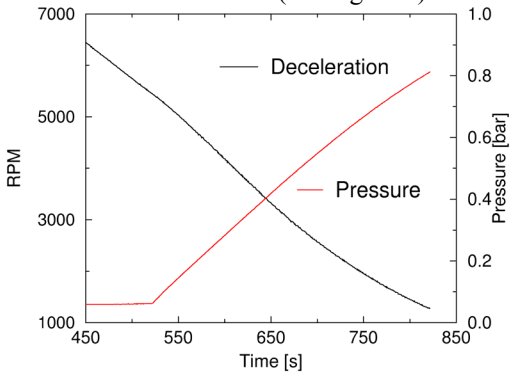

Figure 3: Free rotor deceleration with variable pressure level

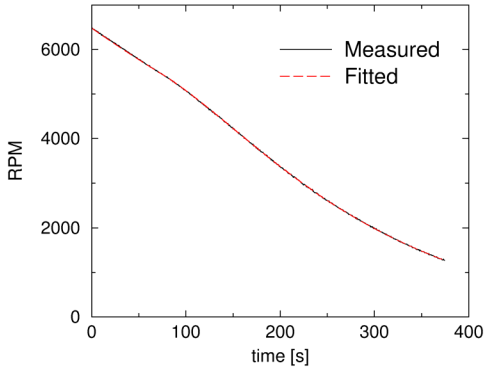

Figure 4: Comparison between the measured deceleration and the prediction.

In order to determine accurately the coefficients $C_{mech}, N_{mech}, C_{vent}, N_{vent}$ in equation 7, a minimization routine from Nag is used that modifies iteratively the coefficients until the predicted deceleration matches the experimental one. Due to the very small contribution of disk windage, the coefficients C_{disk} and N_{disk} are provided by a correlation from Traupel, 1958. The model is able to fit very accurately the measured deceleration as shown in Figure 4. The resulting coefficients are shown in Table 6. They are close to the ones encountered in the literature. The mechanical and windage losses can now be computed. The influence of the axial force that exists during the blowdown tests (but not during the deceleration test) on the mechanical losses is evaluated with correlations provided by the bearing manufacturer. It amounts to about 15% of the

mechanical losses without axial force as shown in Table 7. Note that if the mechanical losses were not taken into account, an overestimation of about 1% is introduced in the efficiency.

	Evaluated	*From literature*
N_{mech}	0.2971	1
C_{mech}	1.4306	1.45
N_{vent}	2.138	2
C_{vent}	$8.74 \cdot 10^{-7}$	$7.8 \cdot 10^{-7}$

Table 6: Comparison between the results of the fit and the coefficients from literature

	0 % condition	*3% condition*
F_{axial} *[N]*	4286	4220
P_{ax} *[kW]*	0.98	0.97
P_{Loss} *[kW]*	14.31	14.29
% of P_{Sh}	0.93 %	0.96 %

Table 7: Axial force and dissipated power in different test conditions.

Enthalpy loss due to heat transfer

Heat is extracted from the fluid due to external convection around the blades and the endwalls. If the heat transfer coefficient h is known, then the convective heat flux can be derived from:

$$\dot{q}_{wall} = h\left(T_{gas} - T_{wall}\right) \qquad (8)$$

- Rotor blades

Didier et al., 2002, performed heat flux measurements on this turbine stage using the thin-film gauge technique on the rotor hub platform, at 15%, 50% and 85 % span and on the blade tip. Some of the results are reported on Figure 5 under the form of a Nusselt number distribution $Nu = hC/k$:

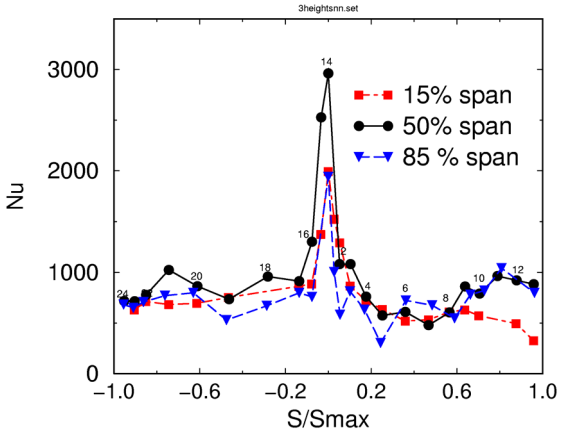

Figure 5: Nusselt number distribution at three different rotor blade heights (Re nom P/P nom).

An integration of the profiles is performed over the blade surface in order to obtain the overall heat absorbed. The same procedure is applied to the hub and tip endwalls. The heat transferred to the rotor casing is calculated from the Nusselt distribution of similar stage, tested with the same Reynolds condition (Chana et al., 2000).

- Stator blades

For the stator blades, there are no heat transfer measurements available. For this reason, measurements performed on a similar geometry (VKI LS89) and tested under similar inlet free stream turbulence (1%), Reynolds number ($Re_{2c}=10^6$) and exit Mach number ($M_{2is}=1.07$) are used (see Figure 6 from Arts and Lambert de Rouvroit, 1992).

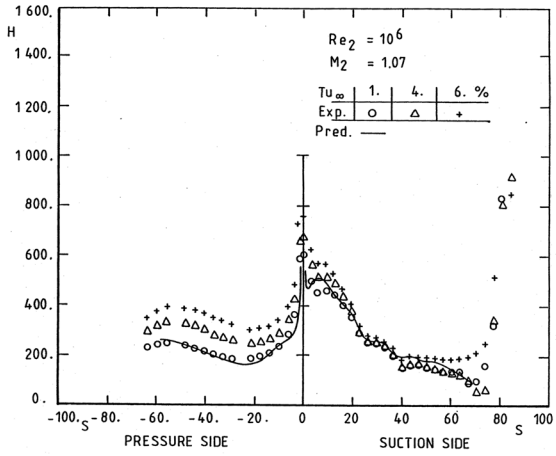

Figure 6: Nusselt distribution for LS89 blade at midspan

The heat transfer to the stator hub and tip endwalls is computed taking a mean value of the Nusselt distribution close to the stator blade trailing edge on pressure side.

-Results

The results of this evaluation are presented in Table 8. Although T_{gas}-T_{wall} is much higher for the stator than for the rotor (for the rotor, the relative total temperature is used for T_{gas}), the rotor receives more heat due to the larger number of blades (64 rotor blades and 43 vanes), thus larger exposed area. The total amount of heat received by the stage in the considered control volume represents more than 3% of the overall power. Clearly, this contribution cannot be neglected.

Stator [kW]	14.65
Rotor [kW]	20.73
Endwalls[kW]	17.56
Total heat[kW]	52.94
% of Power	3.65 %

Table 8: Heat transferred to the blade and endwalls (0% rotor coolant)

Effect of the coolant flows

-Stator coolant flow

The application of the continuity equation on the control volume shown in Figure 1 gives:

$$\dot{m}_{Stator} + \dot{m}_{Cool} = \dot{m}_S + \dot{m}_{leak}$$

Coolant mass flows are measured by means of sonic throats. A complete mixing of the stator mass flow $\dot{m}_{Stator}$ and the coolant flow $\dot{m}_{StatCool}$ is assumed at plane *02*. The enthalpy balance can be written as:

$$\dot{m}_{Stator} CpT_{01} + \dot{m}_{StatCool} CpT_{0C} + P_{Heat} = (\dot{m}_{Stator} + \dot{m}_{StatCool}) CpT_{02mix}$$

resulting in:

$$T_{02mix} = \frac{\dot{m}_{Stator} CpT_{01} + \dot{m}_{StatCool} CpT_{0C} + P_{Heat}}{Cp(\dot{m}_{Stator} + \dot{m}_{StatCool})}$$

-Leakage flow

The leakage flow that exits the turbine stage in between the stator and the rotor platform is supposed to leave the control volume at the temperature T_{02mix}. Therefore, the isentropic power available between planes *01* and *03* is given by the following equation:

$$P_{is} = \dot{m}_{Stator} Cp(T_{01} - T_{03,is}) + \dot{m}_{StatCool} Cp(T_{0C} - T_{03,is}) - \dot{m}_{leak} Cp(T_{02mix} - T_{03,is})$$

The coolant flow has two opposite effects. An increase of the flow rate in the main stream ($\dot{m}_{Stator} + \dot{m}_{Cool}$) corresponds to an increase in the total isentropic power. On the other hand, the cooling down of the main stream decreases the total isentropic enthalpy. Overall, the cooling effect dominates. In the present case (stator coolant mass flow rate of 3% of the stage mass flow), the influence of the coolant flow on the efficiency amounts to 1% and, hence, this contribution cannot be neglected.

-Rotor coolant flow

The rotor is bladed with 64 film-cooled blades. The coolant air enters the disc through axial holes drilled in between the two labyrinth seals (see Figure 7). Finally, a radial duct brings the air to each blade. A rubber seal located between the disc rim and the blade platform prevents leakage. Inside the blade, the coolant air is distributed to the 16 film cooling rows by two internal ducts.

Due to the change of radius between the admission holes and the ejection holes, the rotor acts as a centrifugal compressor and the relative total pressure and temperature of the coolant change. The change in the relative total temperature is estimated thanks to the rothalpy conservation assuming all the coolant flow is ejected through a single hole located at mid-span of the rotor:

$$T_{03rCool} = T_{02rCool} + \frac{U_{3cool}^2}{2Cp} - \frac{U_{2cool}^2}{2Cp}$$

where U_{2coll} and U_{3cool} are the peripheral speeds at the entrance hole and the ejection hole respectively. The change of relative total pressure is computed assuming an isentropic compression. Then, the relative enthalpy of the coolant flow can be mixed with the relative main flow enthalpy in the plane 02:

$$\dot{m}_S T_{02rMix} = \dot{m}_{RotCool} T_{03rCool} + \dot{m}_{Stator} T_{02r}$$

The relative gas temperature T_{02r} is computed from T_{02} using the design velocity triangle:

$$T_{02r} = T_{02} + \frac{w_2^2}{2Cp} - \frac{v_2^2}{2Cp}$$

The new absolute temperature obtained after mixing the rotor coolant flow in the relative frame is obtained with the same design velocity triangle:

$$T_{02Mix} = T_{02rMix} - \frac{w_2^2}{2Cp} + \frac{v_2^2}{2Cp}$$

In this way the change of enthalpy associated with the presence of rotor coolant can be evaluated and taken into account in the evaluation of the power available in the mainstream by performing an isentropic expansion.

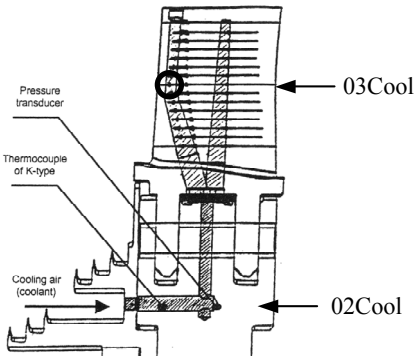

Figure 7: Rotor cooled blade and instrumentation locations

Note that the compression of the air in the disc absorbs shaft power according to:

$$P_{Comp} = \dot{m}_{RotCool}(T_{02rCool} - T_{03rCool})$$

This power should be added in the numerator of equation 4. With the data available, the power P_{Comp} and the overall efficiency are evaluated. The results are presented in Table 9.

The power P_{Comp} is equal to 1.73 kW, less than 0.12 % of the real turbine power. If the rotor coolant flow is taken into account instead of being neglected in the evaluation of the efficiency, a change of only 0.15% is obtained. Therefore it is reasonable to conclude that the influence of the rotor coolant flow can be neglected in this case, owing to the small film cooling mass flow rate (note that the test conditions referred to as 3%

coolant in Table 1 correspond to a real rotor coolant flow rate of 0.78%).

P real [kW]	1506.3
P isentropic [kW]	1675.23
P pumping [kW]	1.73
η *with cooling*	0.8991
η *without cooling*	0.8974
T_{02} *with cooling [K]*	467.05
T_{02} *without cooling [K]*	466.52

Table 9: Comparison between the cooled and uncooled rotor calculation

Uncertainty analysis

An uncertainty analysis is now presented in order to identify the terms that have a large influence on the efficiency accuracy. According to Kline & McClintock, 1953, the overall uncertainty is equal to:

$$\frac{\Delta\eta}{\eta}=\left\{0.996\left(\frac{\Delta I}{I}\right)^2+0.996\left(\frac{\Delta\omega}{\omega}\right)^2+1.76\cdot10^{-3}\left(\frac{\Delta P_m}{P_m}\right)^2\right.$$
$$+1.76\cdot10^{-3}\left(\frac{\Delta P_{Heat}}{P_{Heat}}\right)+0.996\left(\frac{\Delta\dot{\omega}}{\dot{\omega}}\right)^2+\left(\frac{\Delta\dot{m}}{\dot{m}}\right)^2$$
$$\left.+\left(\frac{\Delta T_{01}}{T_{01}}\right)^2+4.8\left(\frac{\Delta\gamma}{\gamma}\right)^2+0.79\left(\frac{\Delta\beta}{\beta}\right)^2\right\}^{0.5} \qquad (5)$$

The coefficients in front of each term of the equation represent the weight of the relative error on the overall relative uncertainty $\Delta\eta/\eta$. Table 10 reports the contribution of the uncertainty of each parameter on the efficiency.

Quantity	*Mean value*	*Absolute uncertainty*	η	$\Delta\eta$ %
I [$kg\ m^2$]	17.704	0.072	0.8721	0.451
$\dot{\theta}$ [*Rpm*]	6490	3	0.8691	0.053
$\ddot{\theta}$ [*Rpm/s*]	1142.2	2.5	0.8709	0.292
P_{Heat} [*kW*]	52.94	0.6	0.86912	0.056
P_{Mech} [*kW*]	14.31	0.4	0.86911	0.054
$\dot{m}_{Cool}[kg/s]$	0.4204	0.004	0.8688	0.013
T_{01} [*K*]	470	2	0.8653	-0.451
P_{01} [*bar*]	2.22	0.005	0.86872	0.003
P_{03} [*bar*]	0.81	0.003	0.8716	0.384
$\dot{m}_S$ [*kg/s*]	15.25	0.24	0.8795	1.24

Table 10: Contribution of each parameter to the overall uncertainty.

The mean value is equal to $\eta=0.8687$ and the overall uncertainty is $\sqrt{\sum(\Delta\eta)^2}=1.44\%$. Observe that the largest influence on the uncertainty is due to the stage mass flow. As mentioned by Porreca and Dénos, 2002, uncertainties of 0.88% were achieved but for other test conditions at lower Reynolds number.

As mentioned earlier, the test-to-test repeatability on mass flow and inertia are lower than the corresponding uncertainties, which means that although the uncertainty on the absolute value remains quite high, variations below the uncertainty can be resolved.

RESULTS

The efficiency is now calculated for a number of tests but only at midspan (equation 5) because, probe pitchwise traverses were not yet performed. It was possible to process a sufficiently large number of tests so that the test-to-test repeatability can be estimated using the standard deviation of each parameter. The results are summarized in Table 11 and Table 12.

0% condition							
	T_{01}	P_{01}	π	$\dot{m}_S$	$\ddot{\theta}$	$\dot{\theta}$	η
Mean	480,7 K	2,221 bar	2,690	15,26 kg/s	1154 rpm/s	6513 rpm	0,876
St. dev	5,372	0,012	0,069	0,030	14,57	15,85	0,020
% St. Dev	1,117	0,527	2,559	0,197	1,263	0,243	2,304
Number of test: 11							

Table 11: Efficiency results for 0% condition

3% condition							
	T_{01}	P_{01}	π	$\dot{m}_S$	$\ddot{\theta}$	$\dot{\theta}$	η
Mean	479,6 K	2,224 bar	2,64	15,36 kg/s	1125 Rpm/s	6517 Rpm	0,865
St. dev	5,76	0,013	0,054	0,033	21,62	16,35	0,020
% St. Dev	1,20	0,608	2,05	0,21	1,92	0,25	2,41
Number of test: 12							

Table 12: Efficiency results for 3% condition

The mean value of the efficiency is equal to 0.876 for the 0% condition and to 0.865 for the 3% condition. In both cases the standard deviation is of the order of 2.4 %. This dispersion is clearly due to the combination of the dispersion of all the quantities needed to compute the efficiency. However some values have more influence than others. It appears, indeed, that the dispersion on the pressure ratio is directly linked to the dispersion on the isentropic power. This drawback is mainly due to the value of the exit pressure P_{03} because the dispersion on the value of the inlet pressure P_{01} is small (only to 0.52 %). As some problems are suspected on the probe or the transducer measuring P_{03}, the pressure P_{04} measured downstream of the

second stator (in this case, the stage was tested in a one and a half stage configuration) will be used instead. In this case, the corrected pressure ratio is calculated in the following way:

$$\pi^* = \frac{P_{01}}{P_{04} + \Delta P_0}$$

where ΔP_0 is the total pressure loss in the second stator and is evaluated taking a mean value between the measured P_{03} and P_{04}. The results are shown in Table 13 and Table 14.

0% condition							
	T_{01}	P_{01}	π^*	$\dot{m}$ Stage	$\ddot{\theta}$	$\dot{\theta}$	η
Mean	480,7 K	2,221 bar	2,751	15,265 kg/s	1154 Rpm/s	6513 Rpm	0,858
St. dev	5,372	0,012	0,023	0,030	14,57	15,85	0,011
% St. Dev	1,11	0,52	0,84	0,19	1,26	0,24	1,35
Number of test: 11							

Table 13: Efficiency for 0% condition calculated with π^*

3% condition							
	T_{01}	P_{01}	π^*	$\dot{m}$ S	$\ddot{\theta}$	$\dot{\theta}$	η
Mean	480,6 K	2,223 bar	2,671	15,36 kg/s	1123 Rpm/s	6520 Rpm	0,851
St. dev	5,124	0,013	0,019	0,034	21,94	14,66	0,011
% St. Dev	1,06	0,625	0,72	0,22	1,95	0,22	1,34
Number of test: 12							

Table 14: Efficiency for 3% condition calculated with π^*

For both conditions, the dispersion on the efficiency is sensibly lower than that computed with the pressure ratio P_{01}/P_{03} (1.34 % instead of 2.34 %) This is the consequence of the lower dispersion on the measurements of P_{04} and, hence, on the corrected pressure ratio π^*. The resulting mean efficiency is equal to 0.858 and 0.851 for 0% and 3% rotor coolant flow conditions respectively. These values are lower than that calculated with the pressure ratio P_{01}/P_{03}. This difference can be attributed to a non-uniform P_{04} in the pitchwise direction. This is due to the presence of the structural struts downstream of the second stator. As a consequence, this local value of P_{04} does not necessarily reflects the pitchwise averaged value.

The acceleration rate also has a non-negligible influence on the efficiency evaluation. This quantity is affecting directly the shaft power and, consequently, the real power given by the fluid to the blades. Larger variations from its mean value correspond to larger variations of the efficiency. A more accurate device for the evaluation of the rotational speed is being designed.

The test-to-test variation on the stage inlet total temperature seems quite high (1.2 %) but this is not influencing significantly the efficiency.

Although results were presented only for the efficiency at mid-span, the integrals of equation 2 can be estimated accurately provided total pressure, total temperature, flow angles and static pressure are measured over the inlet and exit area. The first three quantities can be measured with probe traverses and the last with endwall static pressure taps at hub and tip. To avoid test-to-test dispersion problems, the profiles can be made dimensionless and readapted for each test using the values measured at mid-span. This was not performed here because these quantities were not yet available.

Conclusions

Due to a limited accuracy of thermocouple measurements in a blowdown test rig, the mechanical method is adopted here to evaluate the efficiency.

The determination of efficiency requires evaluating with accuracy a number of quantities, preferably simultaneously to avoid problems of test-to-test repeatability.

The mass flow is of course a key quantity because the uncertainty on the efficiency is directly linked to the one on the mass flow. A specific paper was dedicated to this problem (Porreca and Dénos, 2002). The test-to-test dispersion appears to be below the uncertainty on a single test, i.e. variations smaller than the uncertainty can be measured even if the mean value is not as accurate as wanted.

The shaft power was estimated thanks to the knowledge of the rotor acceleration and inertia. A method to determine the inertia is proposed. Here also, the test-to-test repeatability is below the estimated uncertainty. In practice, a unique value of inertia is used to process all tests and a systematic error is performed that does not affect the capacity of measuring variations.

A method to evaluate mechanical losses and windage losses was developed and used successfully. In this stage, the mechanical losses amount to 1% of the shaft power.

The heat transferred to the blades and the endwall was estimated thanks to heat exchange coefficients measured in a different test campaign. The integration of the heat over all the surfaces results in more than 3% of the shaft power. This contribution can obviously not be neglected.

Finally, the effect of the coolant flows is evaluated. For this stage, the stator coolant mass flow affects noticeably the available power from the fluid (~1% change) while the rotor film-cooling mass flow is so small that it can be neglected.

Finally, results are presented based on mid-span measurements. They demonstrate clearly that if a single key value is not evaluated with accuracy during a test, all others quantities become useless and the efficiency cannot be evaluated with accuracy.

Both the estimated uncertainty for a single test (1.44 %) and the test-to test repeatability (1.35 %) must be improved. Regarding the uncertainty, further work on the mass flow determination will be performed. Regarding the test-to-test repeatability, a pitot rake with kiel heads will be manufactured to improve the accuracy on the downstream stage total pressure. A new system will also be developed that will allow a more accurate determination of the rotor acceleration.

Acknowledgments

The authors want to acknowledge G. Paniagua for the advices given during the study and for the precious help in the determination of the rotor inertia.

References

Arts, T., and Lambert de Rouvroit, M., 1992, "Aerothermal performance of a 2D highly loaded transonic turbine nozzle guide vane – a test case for inviscid and viscous flow computations", *Journal of Turbomachinery*, Vol. 114, no 1, p. 147-154.

Chana K.S. and Mole A.H, 2000 "A summary of cooled NGV and uncooled rotor measurements from the MT1 single stage high pressure turbine in the DERA Isentropic Light Piston Facility (UL)". DERA/AS/PTD/TR000013/1.0.

Didier, F., Dénos, R., and Arts, T., 2002, "Unsteady Rotor Heat Transfer in a Transonic Turbine Stage", ASME paper GT-2002-30195, accepted for publication in the *Journal of Turbomachinery*.

Dénos, R., Arts, T., Paniagua, G.- Michelassi, V., and Martelli, F., 2001, "Investigation of the Unsteady Rotor Aerodynamics in a Transonic Turbine Stage", *Journal of Turbomachinery*, Vol. 123, no 1, pp. 81-89.

Haldemann C., Dunn G., 1996: "*High Accuracy turbine performance measurements in short duration facility*". ASME paper 96-GT-210

Kline S. J. et McClintock F. A. 1953: "*Describing uncertainties in single sample experiments*", Mechanical Engineering, Vol. 75, No 1.

Paniagua, G., Dénos, R., and Arts, T., 2001, "Steady-unsteady Measurements of the Flow Field Downstream of a Transonic HP Turbine Stage", IMechE *Journal of Power and Energy*, vol. 215, pp 663-673.

Paniagua G., 1997, "*Transonic turbine stage performance measurements in a short duration facility and analysis with the 3D N-S Solver of Arnone*", VKI Project Report.

Porreca L. and Dénos R., 2002, "*Turbine stage mass flow evaluation in a compression tube facility*". Proceedings of he 16th symposium on measuring techniques in transonic and supersonic flow in turbomachinery. Cambridge.

Sieverding, C.H. and Arts, T., 1992, "The VKI compression tube annular cascade facility CT3", ASME Paper 92-GT-336.

Traupel W. *Thermische turbomaschinen*, Bd. 1. Springer, Gottingen, Heidelberg 1958